# Pressure and Field Dependence of Superconductivity in $Rb_3C_{60}$

G. Sparn and J. D. Thompson

*Los Alamos National Laboratory, Los Alamos, New Mexico 87545*

R. L. Whetten, S.-M. Huang, R. B. Kaner, and F. Diederich

*Department of Chemistry and Biochemistry and Solid State Science Center, University of California,*
*Los Angeles, California 90024-1569*

G. Grüner and K. Holczer[a]

*Department of Physics and Solid State Science Center, University of California, Los Angeles, California 90024-1569*

Direct measurements of the pressure dependence of the superconducting transition temperature $T_c$ for single-phase $Rb_3C_{60}$ provide for the first time substantial evidence that $T_c$ in $A_3C_{60}$ compounds may be a universal function of the lattice constant (inter-$C_{60}$ spacing). Determination of the lower ($H_{c1}$) and upper ($H_{c2}$) critical fields, and consequently the superconducting penetration depth and coherence length, is also reported. Compared to $K_3C_{60}$, the measured quantities are consistent with a 15% larger electronic-state density in $Rb_3C_{60}$ arising from a greater inter-$C_{60}$ spacing in this compound.

PACS numbers: 74.40.+k, 74.30.Ci

The discovery [1–3] that alkali-buckminsterfullerene compounds form a new family of superconductors has stimulated substantial theoretical and experimental interest. Systematic studies [3–7] of potassium compounds have established that superconductivity appears only in the stoichiometric $K_3C_{60}$ composition [3], which forms an fcc structure [6]. The transition temperature, $T_c = 19.3$ K, decreases strongly with increasing pressure $dT_c/dP = -7.8$ K/GPa [5]. Magnetization measurements [4] have shown $K_3C_{60}$ to be an extreme type-II superconductor with a London penetration depth $\lambda_L = 240$ nm and a superconducting coherence length $\xi_0 = 2.6$ nm. The temperature dependence of the lower critical field $H_{c1}(T)$ and of $\lambda_L(T)$ determined [7] by muon-spin rotation strongly suggests a singlet, $s$ wave pairing. Until now, little has been reported regarding the second member of the family, the superconducting $Rb_3C_{60}$ compound, beyond its transition temperature, $T_c = 29.6$ K [2,3].

Samples were prepared from a solid-phase reaction of high-purity $C_{60}$ powder reacted with Rb vapor in a way similar to that reported for $K_3C_{60}$. As described in detail elsewhere [8], the major difference lies in the kinetics of the solid-gas reaction, which in the case of Rb results in a strong tendency toward segregation of different stoichiometric compounds, independent of the initial ratio of materials used. The sample used in the present work was prepared from a starting composition of $Rb_{2.5}C_{60}$, heated in vacuum at 200°C for 22 h, and subsequently annealed under He atmosphere over several days at the same temperature. This procedure led to a fractional shielding diamagnetism of ca. 25% on powder, determined relative to a Nb bulk reference sample. X-ray diffraction revealed an fcc crystal structure identical to that of $K_3C_{60}$ but with lattice constant 1.4425 nm, compared to 1.4240 nm for $K_3C_{60}$ [8]. The powder was pressed at 4 MPa to make a pellet of 3 mm diam and 0.7 mm thickness, and then sintered at 200°C for 6 h. Pressing also results in

the appearance of bulk shielding (macroscopic supercurrent) at a somewhat lower temperature than $T_c$, similar to that described earlier in the case of pressed $K_3C_{60}$ [5].

Pressure and $H_{c2}(T)$ measurements were performed on a 2.57-mg portion cut from the $Rb_3C_{60}$ pellet sealed under 0.1 MPa He gas in a Pyrex capillary. For reasons to be discussed, $H_{c1}(T)$ was determined on a powder sample also sealed with He in Pyrex. In making measurements with a Quantum Design SQUID magnetometer, care was taken to ensure that the sample was not exposed to a field gradient larger than 0.03% of the applied field. The pressure dependence of $T_c$ was measured inductively at a frequency of 457 Hz, using a self-clamping pressure cell [9] with Fluorinert FC-75 as the hydrostatic pressure medium [5]. For these measurements the sample was removed from the Pyrex capillary and immersed directly into the pressure medium. Pressure within the cell was determined from the variation in $T_c$ of a high-purity lead reference.

Figure 1 shows results of ac susceptibility measurements at a series of pressures between ambient pressure and $P = 1.9$ GPa. In the inset are shown typical susceptibility curves, each exhibiting in addition to the shielding-diamagnetism onset at $T_c$, a second break in slope at $T^* < T_c$, where the macroscopic shielding current is established, i.e., the intergranular coherence appears, as will be described in full detail [10]. A strongly negative pressure dependence is found for both $T_c$ and $T^*$, as displayed in the figure, from which an initial slope $(dT_c/dP)_{P=0} = -9.7$ K/GPa is inferred, an even larger value than that reported for $K_3C_{60}$ (see Table I) [5]. At the highest pressure attempted, $T_c$ is near 13 K, less than half its ambient pressure value. The data points were taken for both increasing and decreasing pressures, demonstrating that the entire variation as a function of pressure is reversible. Additionally, a slight bump is ob-
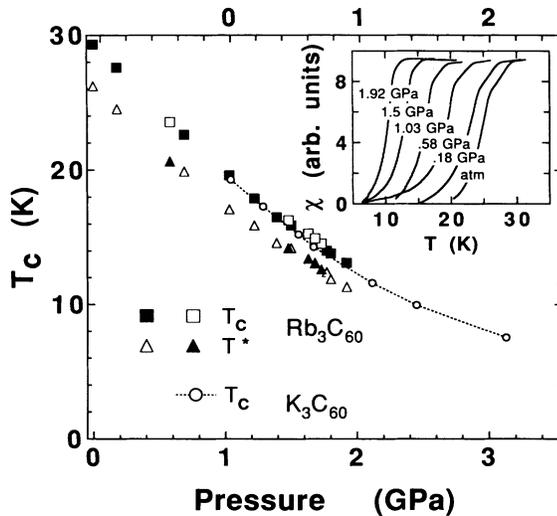
FIG. 1. Inset: Magnetic susceptibility curves $\chi(T;P)$ of $Rb_3C_{60}$ obtained under the indicated pressures at nominal zero magnetic field. The transition temperature $T_c$ (inflection point at highest temperature) and a secondary kink $(T^*)$—not present in unpressed samples and reflective of an intergranular coherence transition—are both clearly visible. The full scale of $\chi$ corresponds to 100% (bulk) diamagnetic shielding. The main plot shows the dependence of $T_c$ and $T^*$, as determined from $\chi(T)$ curves like those in the inset, vs applied pressure. Solid and open symbols correspond to data taken with increasing and decreasing pressure, respectively. For comparison, several points from the $T_c(P)$ curve of $K_3C_{60}$ have been plotted on the same scale but with a $P$ scale translated by 1.06 GPa. Both data sets approximately follow $T_c(P) = T_c(0)\exp(-\gamma P)$, where $\gamma = 0.44 \pm 0.03$ GPa$^{-1}$.

served near 1.5 GPa for both $T_c$ and $T^*$, which is significant and surely not an instrumental artifact. A similar observation has been reported for $V_3Si$ [11], which undergoes a pressure-induced structural transition accompanied by a change in $dT_c/dP$, associated with a soft phonon mode at ambient pressure. This provides further motivation for structural investigation under pressure.

The determination of the lower critical field $H_{c1}$ is complicated when using a compressed pellet because the applied field $H$ first breaks the intergranular supercurrents, leaving the individual grains acting as a powder sample [10]. Figure 2 shows typical magnetization curves $M(H)$ at two different maximum applied fields (0.02 and 5 T), at both $T=5$ K and ambient pressure. Figure 2(a) shows that the intergranular supercurrents are reduced to near zero for $H=20$ mT; whereas Fig. 2(b) shows even at 5 T substantial hysteresis that we associate with intragranular supercurrents. An analysis of the hysteresis, using a critical-state model described in Ref. [4], gives an intragranular critical-current density $J_c = 1.5 \times 10^6$ A/cm² at $H=1$ T and $T=5$ K. This $J_c$ value is about 1 order of magnitude larger than that obtained on $K_3C_{60}$ assuming the same 1-$\mu$m particle size for

TABLE I. Superconductivity parameters in $A_3C_{60}$ compounds.

| Parameter | $A$ = Rb | $A$ = K |
|---|---|---|
| $T_c$ (K) | 29.6 | 19.3 |
| $(dT_c/dP)_{P=0}$ (K/GPa) | $-9.7$ | $-7.8$ |
| $H_{c1}$ (mT) | 12 | 13 |
| $H_{c2}$ (T) | 78 | 49 |
| $H_c$ (T) | 0.44 | 0.38 |
| $J_c$ $(10^5$ A/cm$^2)_{T=5K}$ | 15 | 1.2 |
| $\xi_0$ (nm) | $2^{+0.3}_{-0.2}$ | $2.6^{+0.4}_{-0.2}$ |
| $\lambda_L$ (nm) | $247^{+10}_{-20}$ | $240^{+10}_{-20}$ |
| $\kappa = \lambda_L/\xi_0$ | 124 | 92 |

this material.

Because of the possibility that the intrinsic $H_{c1}$ of $Rb_3C_{60}$ could be masked by intergranular supercurrents at low fields, dc magnetization measurements were also performed on a powder sample prepared as described above. The inset of Fig. 3(a) shows that a flux penetration field $H_a^*$ can be clearly defined by the deviation from linear $M$ vs $H$ behavior. From values of $H_a^*$ determined at various temperatures, we calculate $H_{c1} = H_a^*/(1-n)$, assuming a demagnetization factor $n = \frac{1}{3}$, appropriate to a sphere, which reflects the geometry of isolated $Rb_3C_{60}$ particles. Figure 3(a) gives the temperature dependence of $H_{c1}(T)$ evaluated this way. The zero-temperature extrapolated value of $H_{c1}(0)$ is $12 \pm 3$ mT.

The upper critical field value $H_{c2}$ has been determined from magnetization curves $M(T)$ taken by zero-field cooling to well below $T_c$, applying various fields in the range of 0.2 to 5 T, and recording values by warming the sample to well above $T_c$. Typical magnetization curves for different fields are shown in the inset of Fig. 3(b).
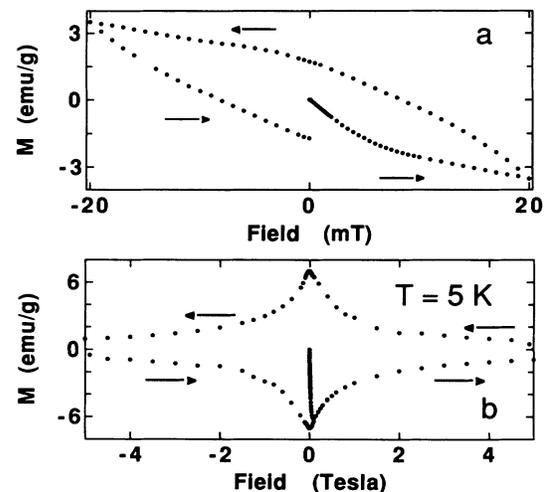


FIG. 2. Representative magnetization curves $M(H)$ recorded at $T=5$ K and ambient pressure, with the field swept as indicated by arrows over two different field ranges: (a) The range $-20$ to $+20$ mT, where the hysteresis loop in the intergranular regime is evident; (b) $M(H)$ at fields to 5 T.
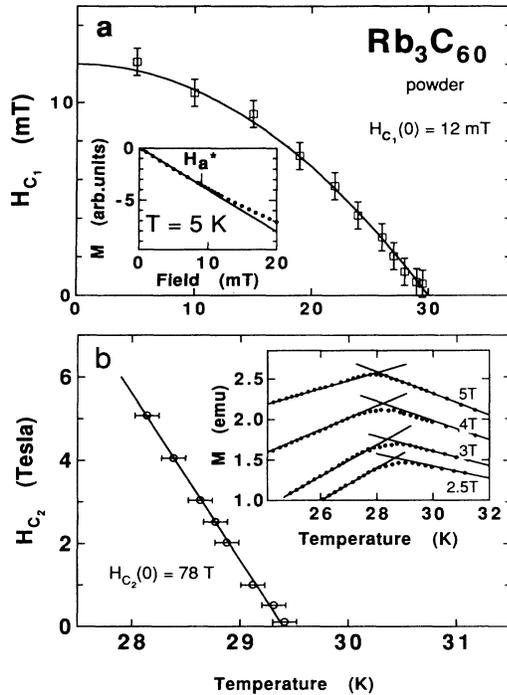
FIG. 3. (a) The temperature dependence of the lower critical field $H_{c1}(T)$ determined on a powder sample as shown in the inset and explained in the text. Error bars represent estimated uncertainty in determining $H_a^*$. The solid line represents the empirical law $H_{c1}(T)/H_{c1}(0) = 1 - (T/T_c)^2$. (b) The temperature dependence of the upper critical field $H_{c2}(T)$. Inset: The method of determining these values from $M(T)$ curves at fixed field. The error bars in the main $H_{c2}(T)$ plot reflect the rounding of the transition.

Note that the transition is somewhat broader than in the case of the $K_3C_{60}$, and might be due to Rb deficiency [8]. $T_c$ is determined from the intercept of linear extrapolations from below and above the transition, as shown. Figure 3(b) shows the $H_{c2}$ values obtained in this way as a function of temperature, along with a linear fit resulting in a critical field slope of $-3.9$ T/K. Using the Werthamer-Helfand-Hohenberg formula [12], a zero-temperature extrapolated value $H_{c2}(0) = 78 \pm 10$ T is obtained. This value exceeds the Pauli weak-coupling limit of 53 T [13].

From $H_{c2}(0)$ and $H_{c1}(0)$, we evaluate the zero-temperature superconducting coherence length $\xi_0$ and London penetration depth $\lambda_L$ using the relations [14]

$$H_{c2}(0) = \Phi_0/2\pi\xi_0^2, \quad H_{c1}(0) = (\Phi_0/4\pi\lambda_L^2)\ln(\lambda_L/\xi_0), \quad (1)$$

where $\Phi_0$ is the flux quantum. We find $\xi_0 = 2^{+0.3}_{-0.2}$ nm and $\lambda_L = 247^{+10}_{-20}$ nm. These values are compared in Table I with values obtained for $K_3C_{60}$. $\xi_0$ for the Rb compound is somewhat smaller than obtained in the case of $K_3C_{60}$ but still larger than the nearest-neighbor $C_{60}$ distance $d$ (ca. 1 nm). We also estimate the thermodynamic critical field from $H_c^2(0) = H_{c1}(0)H_{c2}(0)/\ln\kappa$ (Ref. [14]) and compare it to $K_3C_{60}$ in Table I.

The outstanding question remains as to why $T_c$ for $Rb_3C_{60}$ is over 10 K higher than for $K_3C_{60}$. A notable difference between the two alkali metals is the greater spatial extent of the $5s^1$ configuration of Rb relative to the $4s^1$ configuration of K and consequently a lattice parameter for $Rb_3C_{60}$ that is 0.0185 nm greater than in $K_3C_{60}$ (which interestingly corresponds to the difference in ionic radii) [6]. That is, compared to $Rb_3C_{60}$, $K_3C_{60}$ at ambient pressure is subjected to an effective "chemical" pressure arising from the smaller ionic radius of K. Figure 1 shows that if $T_c(P)$ for $K_3C_{60}$ is shifted rigidly by 1.06 GPa relative to that for $Rb_3C_{60}$, $T_c$'s of both compounds coincide and have essentially the same pressure dependence. This pressure shift, if driven solely by steric effects, should correspond to the chemical pressure calculated from the lattice-parameter difference and the linear compressibility $\kappa$ of $K_3C_{60}$. Unfortunately, $\kappa$ is not known for $K_3C_{60}$. However, assuming a linear compressibility $d(\ln a)/dP = 1.21 \times 10^{-2}$ GPa$^{-1}$ for $K_3C_{60}$ gives the required chemical pressure. This assumed value of $\kappa$ is reasonable given reported values for pure $C_{60}$ that range from $1.8 \times 10^{-2}$ GPa$^{-1}$ (Ref. [15]) to $2.3 \times 10^{-2}$ GPa$^{-1}$ (Ref. [16]). We believe this agreement is not fortuitous but provides an important clue to the mechanism of superconductivity, namely, that $T_c$ is a unique function of volume, i.e., lattice spacing. A naive extrapolation of $T_c$ on the lattice constant $a_0$, using the ionic radius of $Cs^+$, predicts $a_0 = 1.48$ nm and $T_c = 43$ K for $Cs_3C_{60}$.

The straightforward scaling of $T_c$ with the lattice constant suggests that the mechanism responsible for pair formation is intrinsic to the $C_{60}$ molecule and that the dominant pressure-sensitive parameter is the bandwidth which is governed by the overlap between molecules. The ratio of bandwidths, or equivalently state densities $N(0)$ at the Fermi energy, for $Rb_3C_{60}$ and $K_3C_{60}$ can be estimated from the respective $T_c$'s, coherence lengths, and the relation [14] $\xi_0 \propto v_F/T_c$, where in a free-electron model the Fermi velocity $v_F \propto N(0)$. This relationship gives $N(0)_{Rb_3C_{60}} = 1.18 N(0)_{K_3C_{60}}$, if we use values of $\xi_0$ from Table I, or $N(0)_{Rb_3C_{60}} = 1.24 N(0)_{K_3C_{60}}$ assuming $\xi_0$ is derived from the respective Pauli paramagnetic fields. Further, assuming a BCS expression for $T_c = \omega_D \exp[-1/JN(0)]$ and that the pressure dependence of the cutoff frequency $\omega_D$ is negligible, as inferred from $T_c$ scaling with lattice parameter, we find from the ratios of $\partial(\ln T_c)/\partial P$ that $N(0)_{Rb_3C_{60}} = 1.11 N(0)_{K_3C_{60}}$. Thus, the pressure dependences of $T_c$, coherence lengths, and $T_c$'s of $K_3C_{60}$ and $Rb_3C_{60}$ are consistent with a 15% larger state density in $Rb_3C_{60}$ arising from the greater inter-$C_{60}$ spacing in this compound. Further, the slightly larger state density in $Rb_3C_{60}$ is also consistent with a somewhat larger effective electron mass inferred from values of the penetration depth.

This view of superconductivity in fullerenes in which $T_c$ is dominated by a simple volume-dependent electronic state density suggests that models [17] requiring pairing to be mediated by intermolecular vibrational modes that

involve the alkali metal are inappropriate and that an alkali-metal isotope effect should be absent. However, models in which pairing requires the unique properties of $C_{60}$ itself and in which the coupling strength does not vary substantially between $K_3C_{60}$ and $Rb_3C_{60}$ are favored. In these latter cases, it is not possible from our experiments to distinguish between models emphasizing intramolecular vibrational modes [18,19] or purely electronic correlations [20] as the pairing mechanism. Observation of a carbon-isotope effect would favor the former interpretation [18,19]. However, what is clear from measurements [21] of the normal- and superconducting-state magnetic properties of $K_3C_{60}$ is that the electronic state can be modeled by Fermi-liquid behavior in a relatively narrow band and that the effective electron mass is not renormalized strongly by Coulomb correlations. Any viable theory must be able to satisfy these experimental constraints.

*Note added.*—Since this work was completed, Zhou *et al.* [22] measured the compressibility of $K_3C_{60}$ and $Rb_3C_{60}$ and found $d(\ln a)/dP = 1.20 \times 10^{-2}$ and $1.52 \times 10^{-2}$ GPa$^{-1}$, respectively, which validates our assumption. These compressibilities imply logarithmic volume derivatives of $T_c$ of 11 and 7 for $K_3C_{60}$ and $Rb_3C_{60}$, respectively. Furthermore, Fleming *et al.* have arrived indirectly at conclusions similar to ours on the basis of a structure-$T_c$ relation among $A_x A'_{x-3} C_{60}$ alloy compounds [23].

---

[a]Permanent address: Central Research Institute for Physics, P.O. Box 49, h1525 Budapest, Hungary.

[1] A. F. Hebard *et al.*, Nature (London) **350**, 600 (1991); R. C. Haddon *et al.*, *ibid.* **350**, 320 (1991).

[2] M. J. Rosseinsky *et al.*, Phys. Rev. Lett. **66**, 2830 (1991).

[3] K. Holczer *et al.*, Science **252**, 1154 (1991).

[4] K. Holczer *et al.*, Phys. Rev. Lett. **67**, 271 (1991).

[5] G. Sparn *et al.*, Science **252**, 1829 (1991).

[6] P. W. Stephens *et al.*, Nature (London) **351**, 632 (1991).

[7] Y. J. Uemura *et al.*, Nature (London) **352**, 605 (1991).

[8] K. Holczer *et al.* (to be published).

[9] J. D. Thompson, Rev. Sci. Instrum. **55**, 231 (1984).

[10] J. D. Thompson *et al.* (to be published). Similar effects were reported for $K_3C_{60}$ in Ref. [5].

[11] G. Fasol, J. S. Schilling, and B. Seeber, Phys. Rev. Lett. **41**, 424 (1978).

[12] N. R. Werthamer, E. Helfand, and P. C. Hohenberg, Phys. Rev. **147**, 295 (1966).

[13] A. M. Clogston, Phys. Rev. Lett. **9**, 266 (1962).

[14] M. Tinkham, *Introduction to Superconductivity* (McGraw-Hill, New York, 1975).

[15] S. J. Duclos *et al.*, Nature (London) **351**, 380 (1991).

[16] J. E. Fischer *et al.*, Science **252**, 1288 (1991).

[17] F. C. Zhang, M. Ogata, and T. M. Rice, Phys. Rev. Lett. **67**, 3452 (1991).

[18] C. M. Varma, J. Zaanen, and K. Raghavachari, Science **254**, 989 (1991).

[19] M. Schluter *et al.*, Phys. Rev. Lett. **68**, 526 (1992).

[20] S. Chakravarty, M. P. Gelfand, and S. Kivelson, Science **254**, 970 (1991).

[21] W. H. Wong *et al.* (to be published).

[22] O. Zhou *et al.* (to be published).

[23] R. M. Fleming *et al.*, Nature (London) **352**, 797 (1991).